Power-split hybrid transmission energetic and dynamic evaluation program

Pognant-Gros P. [1]; Wasselin T. [2]; Badin F. [1]
IFP
1 : Rond Point de l'échangeur de Solaize, BP3, 69360 Solaize FRANCE
2 : 1&4 avenue de Bois-Préau, 92852 Rueil-Malmaison, FRANCE
philippe.pognant-gros@ifp.fr

Abstract

This paper focuses on the study of hybrid power-split transmission evaluation. The method proposed here is based on a generic formulation of the mechanical part of the transmission. The kinematics and inertia behaviors are introduced via two matrices and detailed for two power-split transmission examples. Then, the powertrain control problem is formulated in two steps: first, the optimal energy management problem is formulated, then, the difficult issue of controlling the transmissions in a multivariable way is explained. Each driving mode is studied because they each correspond to a specific set of objectives. In the last section, we present simulation results that emphasize the energetic and dynamic issues of such transmissions.

I. INTRODUCTION

Car manufacturers and OEMs have carried out many studies in the field of power-split hybrid transmission, (also known as Electric Infinitely Variable Transmission, or E-IVT), for many years. Indeed these architectures have the advantages of both series and parallel configurations for the enhancement of the IC Engine operating area and dynamics, and overall efficiency of the drive train.

The concept of the power split has been widely popularized through the success of the Toyota Hybrid System (THS), developed by Aisin and Toyota and manufactured in more than two millions units by Toyota and then Lexus since 1997. The THS is of the single-mode input-split type and many other solutions have been proposed and tested. These architectures involve additional planetary gear trains, in compound configurations, and clutches to switch from one mode to another and even to enable fixed gear ratios to be implemented in the 2 mode configurations [1, 2, 3].

The aim of these architectures is to improve the overall efficiency of the drive train and especially to optimize the compromise between the speed ratio range – to be maximized – and the amount of power transmitted through the electric components – to be minimized due to its lower efficiency. This reduction of the series' energy path will also enable the maximum power of the electric machine to be decreased and consequently its, cost, size and weight.

However, it appears that E-IVT architecture types are numerous and require specific procedures in order to properly size their components and set up their complex control algorithms. We propose an analytical approach to the feedback control problem of E-IVT and a way to provide set-points in order to minimize the fuel consumption. First of all, we focus on a generic way to model power-split transmissions. Two cases are considered: input-split and compound-split transmissions.

II. MODELING MONOMODE E-IVT POWERTRAINS

Our method was first applied to the most popular E-IVT case of the Toyota Hybrid System which is, from an architectural standpoint, a single-mode input-split powertrain implementing a single epicyclical gearing. We began our work focusing on this simple system, before going further with a compound-split type (single-mode with a dual planetary gearing, elaborated by Renault). To make the comparison between several architectures easier, we used an electrical analogy and considered the different powertrains as quadripoles (figure 1).

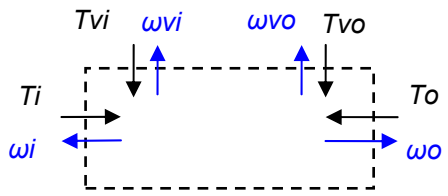

Figure 1. Quadripole input and output convention

The first step to study an E-IVT is the calculation of two basic matrices. The first, M, is the cinematic matrix linking the rotary velocities of electrical machines on the one hand and of the engine and the wheels on the other hand, while the second matrix, J, stands for the inertia effects in the transmission.

Established on the classical Willis relation and some others specific to the studied system (between the different elements of the gear, e.g. ring or sun can be blocked, so the corresponding velocity is null), these matrices are defined according to the two following relations:

978-1-4244-8218-4/10/$26.00 ©2010 IEEE

$$\begin{pmatrix}\omega_i\\ \omega_o\end{pmatrix} = M\begin{pmatrix}\omega_{vi}\\ \omega_{vo}\end{pmatrix} \text{ (1) and } \begin{pmatrix}T_{vi}\\ T_{vo}\end{pmatrix} = J\begin{pmatrix}\dot{\omega}_{vi}\\ \dot{\omega}_{vo}\end{pmatrix} - M^t\begin{pmatrix}T_i\\ T_o\end{pmatrix} \text{ (2)}$$

With R standing for the gearing ratio between ring and sun teeth numbers, the epicyclical gearing is indeed governed by equations (3), (4) and (5).

Willis relation: $(1+R)\omega_c - R\omega_r - \omega_s = 0$ (3)

Gearing torque equations:

$$T_r = -\frac{R}{(1+R)}\cdot T_c = -\beta\cdot T_c \qquad T_s = -\frac{1}{(1+R)}\cdot T_c = -\alpha\cdot T_c \text{ (4) and } \begin{cases} J_s\dot{\omega}_s = T_1 - T_s \\ J_r\dot{\omega}_r = T_2 - T_r \\ J_c\dot{\omega}_c = T_3 - T_c \end{cases} \text{ (5)}$$

Thus, the M and J matrices were calculated for the two previously mentioned powertrains, because they constitute the basis to elaborate an adapted control to pilot these transmissions. These matrices describe the system completely and conform to the definition of the command laws which will be presented in the third part.

A. Input-split type transmission system

The following figure presents the principle scheme of the Toyota Prius powertrain, with a single epicyclical gearing. It is composed of three elements with their own inertia: the sun (J_s), the ring (J_r) and the planet carrier (J_c).

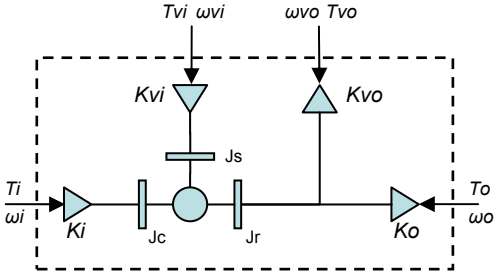

Figure 2. Toyota Prius transmission system scheme

In addition, each quadripole port has its own proportional gain (K) to compute the most generic matrices. After evaluation and with $\alpha = \frac{1}{1+R}$ and $\beta = \frac{R}{1+R}$, the quadripole can be described by the two matrices M and J respectively in equations (6) and (7).

$$M = \begin{pmatrix} \frac{\alpha K_{vi}}{K_i} & \frac{\beta}{K_i K_{vo}} \\ 0 & \frac{K_o}{K_{vo}} \end{pmatrix} \quad (6)$$

$$J = \begin{pmatrix} \left(J_s + J_c\alpha^2\right){K_{vi}}^2 & J_c\frac{\alpha\beta K_{vi}}{K_{vo}} \\ J_c\frac{\alpha\beta K_{vi}}{K_{vo}} & \frac{J_r + J_c\beta^2}{{K_{vo}}^2} \end{pmatrix} \quad (7)$$

We applied it on a more complex powertrain, the compound-split transmission developed by Renault [5].

B. Compound split type transmission system

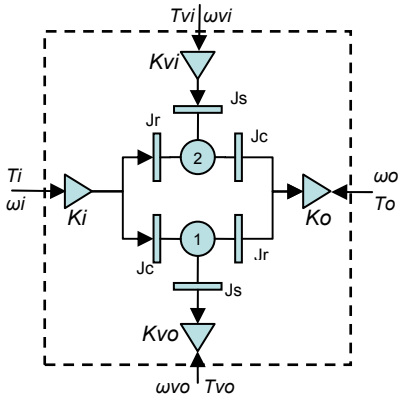

Figure 3. Renault transmission system scheme

Based on a double planetary gearing architecture, represented in figure 3, this configuration is an alternative to the classical Prius THS powertrain. As for the Prius, we first calculated the two matrices M and J. With the increasing complexity of the powertrain comes the same trend on the matrices, even if we recognize the global pattern already seen on the Prius system matrices.

We used a similar convention to represent the Renault transmission, and easily obtained for the M matrix:

$$M = \begin{pmatrix} \frac{\alpha_2\beta_1 K_{vi}}{(1-\beta_1\beta_2)K_i} & \frac{\alpha_1}{(1-\beta_1\beta_2)K_i K_{vo}} \\ \frac{\alpha_2 K_{vi} K_o}{(1-\beta_1\beta_2)} & \frac{\alpha_1\beta_2 K_o}{(1-\beta_1\beta_2)K_{vo}} \end{pmatrix} \quad (8)$$

The calculation of J is here more complex than for the THS. We started with the torque equation for each epicyclical gearing and two relations for the mechanical nodes (A on the thermal engine side and B on the wheel side):

Gear 1:
$$\begin{cases} \frac{J_{S1}}{K_{vo}}\dot{\omega}_{vo} = K_{vo}T_{vo} + \alpha_1 T_{C1} \\ \frac{J_{R1}}{K_o}\dot{\omega}_o = T_{B1} + \beta_1 T_{C1} \\ J_{C1}K_i\dot{\omega}_i = T_{A1} - T_{C1} \end{cases} \quad (9)$$

Gear 2:
$$\begin{cases} J_{S2}K_{vi}\dot{\omega}_{vi} = \frac{T_{vi}}{K_{vi}} + \alpha_2 T_{C2} \\ J_{R2}K_i\dot{\omega}_i = T_{A2} + \beta_2 T_{C2} \\ J_{C2}\frac{\dot{\omega}_o}{K_o} = T_{B2} - T_{C2} \end{cases} \quad (10)$$

Nodes A and B:
$$\begin{cases} \frac{T_i}{K_i} - T_{A1} - T_{A2} = 0 \\ K_o T_o - T_{B1} - T_{B2} = 0 \end{cases} \quad (11)$$

Then we substituted the node torques T_A and T_B in (11) with their expression from (9) and (10). In addition, with the last unused equations, we evaluated the torques T_C:

$$\begin{cases} K_o T_o + \beta_1 T_{C1} - T_{C2} - (J_{R1} + J_{C2}) \dfrac{\dot{\omega}_o}{K_o} = 0 \\ \dfrac{T_i}{K_i} - T_{C1} + \beta_2 T_{C2} - (J_{R2} + J_{C1}) K_i \dot{\omega}_i = 0 \end{cases} \quad (12)$$

$$\begin{cases} T_{C1} = -\dfrac{K_{vo}}{\alpha_1} T_{vo} + \dfrac{J_{S1}}{\alpha_1 K_{vo}} \dot{\omega}_{vo} \\ T_{C2} = -\dfrac{T_{vi}}{\alpha_2 K_{vi}} + \dfrac{J_{S2} K_{vi}}{\alpha_2} \dot{\omega}_{vi} \end{cases} \quad (13)$$

We thus obtained, replacing the torques T_C in (12) by their value (13):

$$\begin{cases} \dfrac{T_i}{K_i} + \beta_2 K_o T_o - (1 - \beta_1 \beta_2) T_{C1} - (J_{R2} + J_{C1}) K_i \dot{\omega}_i - \dfrac{(J_{R1} + J_{C2}) \beta_2}{K_o} \dot{\omega}_o = 0 \\ \dfrac{\beta_1}{K_i} T_i + K_o T_o - (1 - \beta_1 \beta_2) T_{C2} - (J_{R2} + J_{C1}) \beta_1 K_i \dot{\omega}_i - \dfrac{(J_{R1} + J_{C2})}{K_o} \dot{\omega}_o = 0 \end{cases} \quad (14)$$

Finally, with the equation (1), we substituted ω_i and ω_o by ω_{vi} and ω_{vo}:

$$\begin{cases} T_{vi} = -m_{11} T_i - m_{21} T_o + \left(J_{S2} K_{vi}^{\ 2} + (J_{R2} + J_{C1}) m_{11}^{\ 2} K_i^{\ 2} + (J_{R1} + J_{C2}) \dfrac{m_{21}^{\ 2}}{K_o^{\ 2}} \right) \dot{\omega}_{vi} \\ \quad \ldots + \left((J_{R2} + J_{C1}) m_{11} m_{12} K_i^{\ 2} + (J_{R1} + J_{C2}) \dfrac{m_{21} m_{22}}{K_o^{\ 2}} \right) \dot{\omega}_{vo} \\ T_{vo} = -m_{12} T_i - m_{22} T_o + \left((J_{R2} + J_{C1}) m_{11} m_{12} K_i^{\ 2} + (J_{R1} + J_{C2}) \dfrac{m_{21} m_{22}}{K_o^{\ 2}} \right) \dot{\omega}_{vi} \\ \quad \ldots + \left(\dfrac{J_{S1}}{K_{vo}^{\ 2}} + (J_{R2} + J_{C1}) m_{12}^{\ 2} K_i^{\ 2} + (J_{R1} + J_{C2}) \dfrac{m_{22}^{\ 2}}{K_o^{\ 2}} \right) \dot{\omega}_{vo} \end{cases} \quad (15)$$

And we were able to express the matrix J as defined in equation (2):

$$J = \begin{pmatrix} j_{11} & j_{12} \\ j_{21} & j_{22} \end{pmatrix}$$

avec

$$j_{11} = J_{S2} K_{vi}^{\ 2} + (J_{R2} + J_{C1}) m_{11}^{\ 2} K_i^{\ 2} + (J_{R1} + J_{C2}) \frac{m_{21}^{\ 2}}{K_o^{\ 2}}$$

$$j_{12} = (J_{R2} + J_{C1}) m_{11} m_{12} K_i^{\ 2} + (J_{R1} + J_{C2}) \frac{m_{21} m_{22}}{K_o^{\ 2}}$$

$$j_{21} = (J_{R2} + J_{C1}) m_{11} m_{12} K_i^{\ 2} + (J_{R1} + J_{C2}) \frac{m_{21} m_{22}}{K_o^{\ 2}}$$

$$j_{22} = \frac{J_{S1}}{K_{vo}^{\ 2}} + (J_{R2} + J_{C1}) m_{12}^{\ 2} K_i^{\ 2} + (J_{R1} + J_{C2}) \frac{m_{22}^{\ 2}}{K_o^{\ 2}} \quad (16)$$

C. *Full powertrain model*

In this part, we derived a powertrain state-space model with torque actuator inputs. Figure 4 presents the hybrid powertrain with its transmission and its actuators: an engine and 2 electric machines.

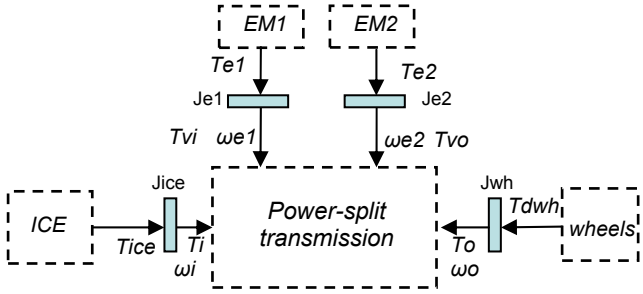

Figure 4. Powertrain

It is possible to obtain a simple equation to describe the bahevior of each new component.

Ignition Combustion Engine (ICE):

$$J_{ice} \dot{\omega}_{ice} = T_{ice} - T_i + T_{dice} \quad (17)$$

where T_{dice} represents the engine friction torque and T_{ice} the effective engine torque calculated by the powertrain control.

Electric machines 1 and 2 (EM1,2):

$$J_e \begin{bmatrix} \dot{\omega}_{e1} \\ \dot{\omega}_{e2} \end{bmatrix} = \begin{bmatrix} T_{e1} \\ T_{e2} \end{bmatrix} - \begin{bmatrix} T_{vi} \\ T_{vo} \end{bmatrix} \quad (18)$$

where J_e is the diagonal matrix of electric machines rotor inertia J_{e1} and J_{e2}. Note that the electric machines speeds ω_{e1} and ω_{e2} are assumed to be the only measurements in the following.

Wheels:

$$J_{wh} \dot{\omega}_{wh} = -T_o + T_{dwh} \quad (19)$$

where: $J_{wh} = J_{axle} + m_{vehicle} R_{wheel}^{\ 2}$

and $T_{dwh} = -\rho S C_x V_{vh}^{\ 2} \cdot R_{wheel} - d$

T_{dwh} is the sum of all friction torques applied to the longitudinal dynamic of the vehicle.

From (1), (2), (17), (18), (19), a state-space model of the powertrain is deduced:

$$\begin{cases} \bar{J}_e \dot{\omega}_e = T_e + M^t \begin{bmatrix} T_{ice} + T_{dice} \\ T_{dwh} \end{bmatrix} \\ \omega_{ice} = [1 \quad 0] M \omega_e \\ \begin{bmatrix} T_i \\ T_o \end{bmatrix} = \begin{bmatrix} T_{dice} \\ T_{dwh} \end{bmatrix} - J_{wh} M \dot{\omega}_e \end{cases} \quad (20)$$

with $\bar{J}_e = \begin{bmatrix} J_{e1} & 0 \\ 0 & J_{e2} \end{bmatrix} + J + M^T \begin{bmatrix} J_{ice} & 0 \\ 0 & J_{wh} \end{bmatrix} M$

and $J_{wh} = \begin{bmatrix} J_{ice} & 0 \\ 0 & J_{wh} \end{bmatrix}$

D. *Electric part model*

An example of electric part architecture is described in figure 5.

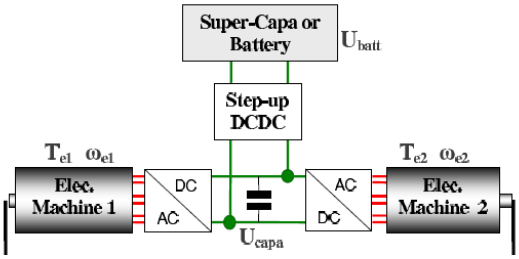

Figure 5. Electric part example description

Electric power conservation is given by:

$$\dot{E}_{capa} = -\omega_e^t T_e - P_{loss} + P_{dcdc} \qquad (21)$$

where P_{loss} represents the sum of both electric machines (+inverters) losses, as a function of speed and torque. P_{dcdc} is the electric power from the energy storage system to the electric machines. In the following, we assume that the energy storage system is a battery.

III. CONTROL STRATEGIES OF SINGLE-MODE E-IVT POWERTRAINS

This step of the study deals with the control of a hybrid vehicle powertrain composed of an E-IVT transmission. Such a powertrain can operate in four different modes: hybrid, electric drive, start engine and stop engine. In each case, the available actuators operate to achieve a specific objective. The hybrid mode is the most difficult. The control problem is 3 by 3: 3 objectives (ω_i^{sp} (engine speed), T_o^{sp} (wheel torque) and P_{bat}^{sp}). Some LPV (Linear Parameter Varying) approaches exist [7] but do not lead to an analytical formulation. Here, we propose a non-linear control approach based on a Kalman filter estimator, using (7). In fact, E-IVT architectures allow us to estimate this variable and many others, inside the mechanical part of the transmission. Equations of the whole control law are given as functions of *M* and *J* matrices.

A. *Hybrid mode*

In this mode, the control problem can be split into two parts. The first aims at calculating an optimal operating point satisfying the driver acceleration request and minimizing the fuel consumption. This can be done using a classical static formulation from previous dynamic models. The output of this first control level is a vector of three set-points, basically a wheel torque set-point T_o^{sp}, an engine speed set-point ω_i^{sp} and a battery power set-point P_{bat}^{sp}. The second part, the feedback part, calculates the torque commands in order to track the targets of the first level. To be realistic, this feedback part is essential for such transmissions. It must achieve the maximal decoupling behavior between the three objectives. For example, if the driver wants to accelerate and the optimal engine speed does not vary, the control has to follow the wheel torque target without impacting the low-CO_2 engine speed. Moreover, we aim at decoupling completely the electric objective (P_{bat}^{sp}) from the mechanical objectives (T_o^{sp}, ω_i^{sp}). The only measured variables are the two electrical machines speeds and the voltage of the buffer capacitor linking the two DC-links of the machines.

First control level: Optimal set-point calculation

The main property of E-IVT transmissions is the capability to decouple the engine speed from the wheel speed. The engine speed can be controlled in order to minimize the CO_2 emissions taking into account electrical losses. Thus, the battery power is a second degree of freedom fixing the variator operating point, and the capacity to charge or discharge the battery. For power-split transmissions, at each time, an optimal engine speed set-point ω_i^{sp} and an optimal battery power set-point P_{bat}^{sp} *are* calculated as a function of the vehicle speed and the wheel torque target. To do this a static from of equation was considered [8].

$$\min_{\omega i, Pbat} \left\{ J(\omega i, Pbat) := \int_0^T \dot{m}_{fuel}\left(\omega i, F(\omega i, Pbat, \omega o, To)\right) dt \right\}$$
$$SOC(0) = SOC(T)$$

where $\dot{m}_{fuel}(\omega i, Ti)$ is the instantaneous flow fuel, *SOC* the State of charge of the energy storage system. F(.) is the input torque T_i. In fact, the static equations derived from (2), (18) and (21) allows us to write an implicit function of T_i: $G(Ti, \omega i, Pbat, \omega o, To) = 0$. G(.) only depends on the matrix M and the electric losses.

Applying Pontryagin's minimum principle, minimizing CO_2 emissions tends to minimize at each time the Hamiltonian [8]:

$$H(\omega i, Pbat) = Pfuel(\omega i, F(\omega i, Pbat, \omega o, To)) + sPbat \qquad (22)$$

where P_{fuel} is the instantaneous fuel power. For a given operating point T_o, ω_o, and a given s, it is possible to calculate the optimal set-points ω_{isp}, P_{bat}^{sp} minimizing (22), subject to actuator torque limits and battery power limit. In a pure transmission case (P_{bat}=0), figure 6 presents the map of ωisp as a function of $-T_o$ and ω_o (in km/h) obtained by solving (22).

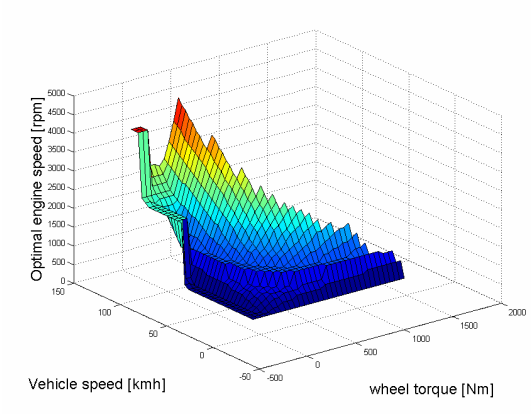

Figure 6. Optimal engine speed for a compound-split transmission

For online implementation purposes, a calculation of s(t) can be used as described in [8].

Second control level: multivariable feedback control

The second part of the powertrain control aims at calculating the torque actuators (for the engine and the two electric machines), in order to achieve simultaneously a mechanical objective and an electrical objective. The mechanical problem is the tracking of the wheel torque target T_o^{sp} and the optimal engine speed set-point ω_i^{sp}. The electrical problem is the tracking of the optimal battery power set-point P_{bat}^{sp}. Both sets of objectives must achieve a decoupled behavior. First, we can separate the electric control from the mechanical control.

To do this, we defined the following variable change for the electric torques.

$$\begin{bmatrix} T_{e1} \\ T_{e2} \end{bmatrix} = \begin{bmatrix} -\dfrac{\omega_{e1}}{\|\omega_e\|^2} & \dfrac{\omega_{e2}}{\Omega} \\ -\dfrac{\omega_{e2}}{\|\omega_e\|^2} & \dfrac{\omega_{e1}}{\Omega} \end{bmatrix} \begin{bmatrix} u_w \\ u_o \end{bmatrix} = D(\omega_e) \begin{bmatrix} u_w \\ u_o \end{bmatrix} \quad (23)$$

$$with\ \Omega = \sqrt{\left(\omega_{e1}{}^{\max}\right)^2 + \left(\omega_{e2}{}^{\max}\right)^2}\ .$$

$D(\omega_e)$ is non singular for all $\omega_e \neq 0$, which is already the case in hybrid mode from (1), since the engine is started. Inverting (23) leads to $u_w = -\omega_e^t \cdot T_e$.

Assuming that the DCDC controls the buffer capacitor voltage U_{capa} at a constant value with a high bandwidth faced to u_w, (21) becomes:

$$u_w = -P_{bat} + P_{loss}$$

Then, u_w can control P_{bat} to P_{bat}^{sp} using a feedback control law. P_{loss} is considered as an unknown disturbance. There is no issue to design a controller. For example, a PI controller can be designed in order to reject P_{loss}, assuming that P_{loss} is a slow varying disturbance:

$$u_w = k_p \int (P_{bat} - P_{bat}{}^{sp}) - P_{bat}{}^{sp} \quad (24)$$

The tuning of kp (kp > 0) allows the electric control bandwidth, which is independent of the mechanical control bandwidth, to be fixed. The mechanical control problem is now presented.

The variable change (23) was calculated using the set of equations (20). For the first equation, we obtained:

$$J_e \frac{d\omega_e}{dt} = \begin{bmatrix} -\dfrac{\omega_{e1}}{\|\omega_e\|^2} & \dfrac{\omega_{e2}}{\Omega} \\ -\dfrac{\omega_{e2}}{\|\omega_e\|^2} & \dfrac{\omega_{e1}}{\Omega} \end{bmatrix} \begin{bmatrix} u_w \\ u_o \end{bmatrix} + M^t \begin{bmatrix} T_{ice} + T_{dice} \\ T_{dwh} \end{bmatrix}$$

$$J_e \frac{d\omega_e}{dt} = \begin{bmatrix} -\dfrac{\omega_{e2}}{\Omega} & M^t \begin{bmatrix} 1 \\ 0 \end{bmatrix} \\ \dfrac{\omega_{e1}}{\Omega} & \end{bmatrix} \begin{bmatrix} u_0 \\ T_{ice} \end{bmatrix} - \frac{\omega_e u_w}{\|\omega_e\|^2} + M^t \begin{bmatrix} T_{dice} \\ T_{dwh} \end{bmatrix}$$

The wheel torque can be expressed as follows, using the variable change (23) and the previous relation:

$$\begin{aligned} T_o &= \begin{bmatrix} 0 & 1 \end{bmatrix} \left(-J_{iw} \frac{d}{dt} \begin{bmatrix} \omega_{ice} \\ \omega_{wh} \end{bmatrix} + \begin{bmatrix} T_{ice} + T_{dice} \\ T_{dwh} \end{bmatrix} \right) \\ &= \begin{bmatrix} 0 & 1 \end{bmatrix} \left(-J_{iw} M \frac{d\omega_e}{dt} + \begin{bmatrix} 1 \\ 0 \end{bmatrix} T_{ice} + \begin{bmatrix} T_{dice} \\ T_{dwh} \end{bmatrix} \right) \\ &= \begin{bmatrix} 0 & 1 \end{bmatrix} \left(\left(I_2 - J_{iw} M J_e^{-1} M^t \right) \begin{bmatrix} T_{ice} + T_{dice} \\ T_{dwh} \end{bmatrix} - \frac{1}{\Omega} J_{iw} M J_e^{-1} \begin{bmatrix} -\omega_{e2} \\ \omega_{e1} \end{bmatrix} u_o + J_{iw} M J_e^{-1} \frac{\omega_e}{\|\omega_e\|^2} u_w \right) \\ &= \begin{bmatrix} 0 & 1 \end{bmatrix} \begin{pmatrix} \left[-\frac{1}{\Omega} J_{iw} M J_e^{-1} \begin{bmatrix} -\omega_{e2} \\ \omega_{e1} \end{bmatrix} \quad \left(I_2 - J_{iw} M J_e^{-1} M^t \right) \begin{bmatrix} 1 \\ 0 \end{bmatrix} \right] \begin{bmatrix} u_o \\ T_{ice} \end{bmatrix} + J_{iw} M J_e^{-1} \frac{\omega_e}{\|\omega_e\|^2} u_w \\ + \left(I_2 - J_{iw} M J_e^{-1} M^t \right) \begin{bmatrix} T_{dice} \\ T_{dwh} \end{bmatrix} \end{pmatrix} \end{aligned} \quad (25)$$

The engine speed dynamic becomes:

$$\dot{\omega}_{ice} = \begin{bmatrix} 1 & 0 \end{bmatrix} M J_e^{-1} \left(\begin{bmatrix} -\dfrac{\omega_{e2}}{\Omega} & M^t \begin{bmatrix} 1 \\ 0 \end{bmatrix} \\ \dfrac{\omega_{e1}}{\Omega} & \end{bmatrix} \begin{bmatrix} u_0 \\ T_{ice} \end{bmatrix} - \frac{\omega_e u_w}{\|\omega_e\|^2} + M^t \begin{bmatrix} T_{dice} \\ T_{dwh} \end{bmatrix} \right) \quad (26)$$

The following matrices were introduced to obtain a compact formulation:

$$K_1 = \frac{1}{\Omega} \begin{bmatrix} \begin{bmatrix} 1 & 0 \end{bmatrix} M \\ \begin{bmatrix} 0 & -1 \end{bmatrix} J_{iw} M \end{bmatrix} J_e^{-1} \begin{bmatrix} 0 & -1 \\ 1 & 0 \end{bmatrix}$$

$$K_3 = \begin{bmatrix} -\begin{bmatrix} 1 & 0 \end{bmatrix} M \\ \begin{bmatrix} 0 & 1 \end{bmatrix} J_{iw} M \end{bmatrix} J_e^{-1}$$

$$K_2 = \begin{bmatrix} \begin{bmatrix} 1 & 0 \end{bmatrix} M J_e^{-1} M^t \\ \begin{bmatrix} 0 & 1 \end{bmatrix} \left(I_2 - J_{iw} M J_e^{-1} M^t \right) \end{bmatrix} \begin{bmatrix} 1 \\ 0 \end{bmatrix}$$

$$K_4 = \begin{bmatrix} \begin{bmatrix} 1 & 0 \end{bmatrix} M J_e^{-1} M^t \\ \begin{bmatrix} 0 & 1 \end{bmatrix} \left(I_2 - J_{iw} M J_e^{-1} M^t \right) \end{bmatrix}$$

If we want to impose a dynamic as follows:

$$\begin{cases} \dot{\omega}_{ice} = k_p\left(\omega_{ice}{}^{sp} - \omega_{ice}\right) = r_1 \\ T_o = T_o{}^{sp} = r_2 \end{cases}$$

then, (25) and (26) can be written in a compact form:

$$\begin{bmatrix} K_1\omega_e & K_2 \end{bmatrix}\begin{bmatrix} u_o \\ T_{ice} \end{bmatrix} = \begin{bmatrix} r_1 \\ r_2 \end{bmatrix} - K_3\frac{\omega_e}{\|\omega_e\|^2}u_w - K_4\begin{bmatrix} T_{dice} \\ T_{dwh} \end{bmatrix}$$

Then, the mechanical control vector can be expressed as:

$$\begin{bmatrix} u_o \\ T_{ice} \end{bmatrix} = \begin{bmatrix} K_1\omega_e & K_2 \end{bmatrix}^{-1}\left\{\begin{bmatrix} k_p\left(\omega_{ice}{}^{sp} - \omega_{ice}\right) \\ T_o{}^{sp} \end{bmatrix} - K_3\frac{\omega_e}{\|\omega_e\|^2}u_w - K_4\begin{bmatrix} T_{dice} \\ T_{dwh} \end{bmatrix}\right\} \quad (27)$$

where u_w comes from the energetic control and is a known signal. Nevertheless, the disturbances T_{dwh} and T_{dice} are not measured. So, based on the linear model (20), we can design an observer in order to provide $\begin{bmatrix} \hat{T}_{dice} \\ \hat{T}_{dwh} \end{bmatrix}$ a vector of estimated disturbances. To this purpose, (20) can be transformed into:

$$\dot{X} = \begin{bmatrix} \dot{w}_e \\ \dot{T}_{dice} \\ \dot{T}_{dwh} \end{bmatrix} = \begin{bmatrix} 0_2 & \bar{J}_e{}^{-1}M^t \\ 0_2 & 0_2 \end{bmatrix}X + \begin{bmatrix} \bar{J}_e{}^{-1} & \bar{J}_e{}^{-1}M^t\begin{bmatrix} 1 \\ 0 \end{bmatrix} \\ 02 & \begin{bmatrix} 0 \\ 0 \end{bmatrix} \end{bmatrix}\begin{bmatrix} T_e \\ T_{ice} \end{bmatrix}$$

$$\begin{aligned} \dot{X} &= AX + Bn \\ \omega_e &= \begin{bmatrix} I_2 & 0_2 \end{bmatrix}X = CX \end{aligned} \quad (28)$$

The observability matrix is structurally of rank 4 if $\bar{J}_e{}^{-1}M^t$ is invertible. By considering the commands T_e and T_{ice}, and the measures of electric motors speeds ω_e, a Kalman filter was designed.

Finally, from (28), the mechanical control equation is:

$$\begin{bmatrix} u_o \\ T_{ice} \end{bmatrix} = \begin{bmatrix} K_1\omega_e & K_2 \end{bmatrix}^{-1}\left\{\begin{bmatrix} k_p\left(\omega_{ice}{}^{sp} - \omega_{ice}\right) \\ T_o{}^{sp} \end{bmatrix} - K_3\frac{\omega_e}{\|\omega_e\|^2}u_w - K_4\begin{bmatrix} \hat{T}_{dice} \\ \hat{T}_{dwh} \end{bmatrix}\right\} \quad (29)$$

The feedback control law which achieves the target specifications $T_o{}^{sp}$, $\omega_i{}^{sp}$, *and* $P_{bat}{}^{sp}$, can be summarized as the synthesis of a Kalman filter based on the model (28), the calculation of an energetic command u_w from (24), the calculation of $\begin{bmatrix} u_0 \\ T_{ice} \end{bmatrix}$ from (29). Then, electric torques T_e were obtained from the variable change (23).

ZEV mode

In this mode, both electric machines must co-operate in order to accelerate the vehicle. Moreover, in this mode, the engine is stopped and the control has to block the crankshaft in order to minimize engine friction torque, but also to prepare the engine for a possible start if needed. These two objectives are equivalent to controlling the wheel torque T_o to $T_o{}^{sp}$, and the transmission input torque T_i to $T_i{}^{sp}$ =0. The condition to enter the ZEV mode control is that the engine must be stopped.

From (20), it is possible to express T_e as a function of the control objectives:

$$T_e = -\bar{J}_e M^{-1}J_{wh}{}^{-1}\begin{bmatrix} T_i{}^{sp} \\ T_o{}^{sp} \end{bmatrix} + \left(\bar{J}_e M^{-1}J_{wh}{}^{-1} - M^t\right)\begin{bmatrix} \hat{T}_{dice} \\ \hat{T}_{dwh} \end{bmatrix} \quad (30)$$

Here, $\begin{bmatrix} \hat{T}_{dice} \\ \hat{T}_{dwh} \end{bmatrix}$ are provided by the same Kalman filter described in the previous hybrid mode part; the only difference is the fact that T_{ice}=0.

START and STOP modes

Starting the engine without wheel lag torque, is equivalent to controlling the wheel torque at the driver's request and simultaneously the torque T_i in order to crank the engine. Once the engine speed reaches a specified value, the hybrid mode is activated. The start mode control objective can be the same as the ZEV mode, except that $T_i{}^{sp} > 0$. So, equation (30) describes the start mode control law.

The approach for the stop mode is the same. Stopping the engine means controlling the engine speed from its current value to 0. Since the engine is in fuel cut-off before stopping it, T_{ice} is no longer a torque command. We must control T_i to a reference $T_i{}^{sp} < 0$. Simultaneously, the wheel torque has to be controlled to satisfy the driver's request. Equation (30) is used again to design the stop mode control.

IV. DYNAMIC AND ENERGETIC EVALUATION

In this section we consider a compound split transmission as depicted in section 1. To initiate the procedure we have considered the drivetrain components as being identical to those of the Prius THSII (with 2 identical planetary gears). To establish the control laws of the drivetrain we have kept the same values for K_i, K_o, K_{vi}, K_{vo}. The vehicle has the same characteristics as the Prius 2 one (mass, electric machines, engine, battery) [4].

The driving cycle used to validate our control is a part of the European driving schedule with it's urban and extra urban characteristics. All the simulations were carried out with an initial battery State of Charge of 60%. In both ZEV mode and hybrid mode, we illustrate the control objectives presented in the previous section.

ZEV mode

First, the wheel torque tracking and T_i tracking are presented. It satisfies equation (30).

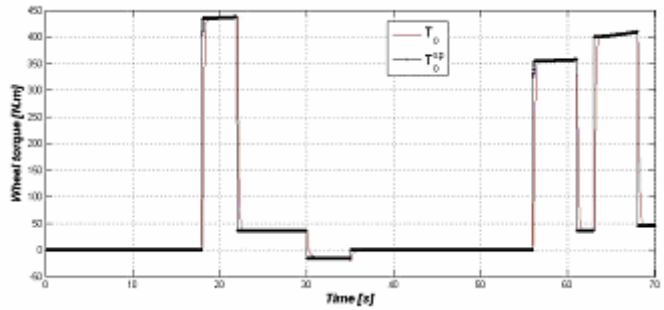

Figure 7. Wheel torque tracking in ZEV mode

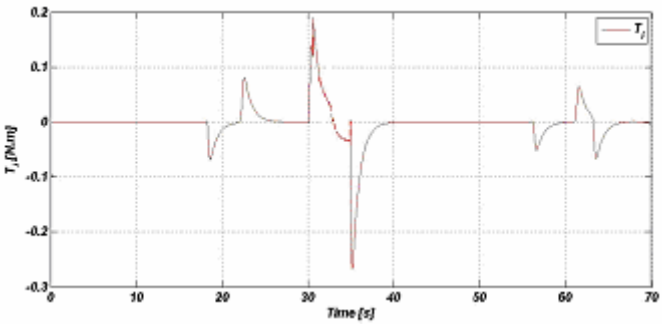

Figure 8. Engine torque regulation in ZEV mode

Hybrid mode

The engine speed and wheel torque control from equation (29) give the following results.

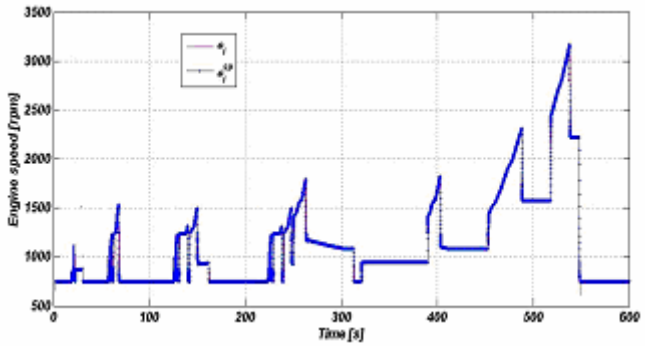

Figure 9. Engine speed tracking in hybrid mode

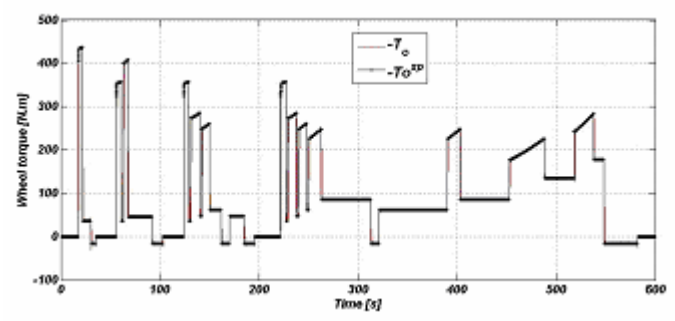

Figure 10. Wheel torque tracking in hybrid mode

We notice that the control objectives are well decoupled. The wheel torque in figure 10 is not disturbed by the engine speed control and vice versa.

Energetic evaluation

The principle of an E-IVT is to divert some of the power delivered by the thermal engine from the direct mechanical path towards the wheels to the electrical path with the battery and the electrical machines. To illustrate this, we present in the following table different set-points, where the power is diverted in varying degrees between the two paths. We chose a stabilized set-point at 50km/h, and another one at 100km/h, both on the EUDC part of the NEDC cycle.

	50 km/h	100 km/h
ICE Power [kW]	5.41	18.22
ME1 Power [kW]	-1.22	-7.77
ME2 Power [kW]	-1.06	3.38
"Wheel" Power [kW]	-3.13	-13.83

Table 1: Power balance in the E-IVT for two stabilized vehicle speeds from the NEDC driving schedule

We notice that for the 50km/h case, the selected engine power to get a minimum fuel consumption on the entire driving schedule is higher than the required power to propel the vehicle, which allows the two electrical machines to work as generators, charging the battery which has been discharged during the urban part of the cycle. On the contrary, at 100km/h, completing the torque and speed demand on the wheel, whilst maintaining the battery State of Charge, required additional torque from the second electrical machine and a strong regeneration from the first one.

The following figures show the speeds and the torques of the three machines (thermal engines and electrical machines) for the NEDC cycle end (ECE + EUDC). The two set-points, previously mentioned correspond to the situation at 370s (50km/h) and 515s (100km/h).

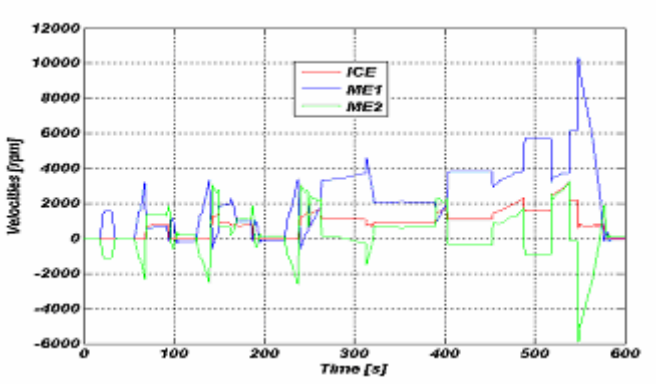

Figure 11. Engine and electrical machines speeds [rpm]

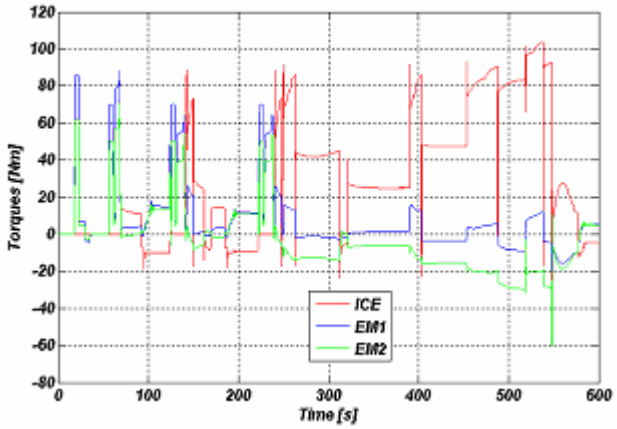

Figure 12. Engine and electrical machines torques [Nm]

V. CONCLUSION

We have presented in this paper a generic method to model and control hybrid power-split transmissions. The different steps of the study concern the M/J model, and computations of optimal maps of set-points that minimize the fuel consumption. Then, analytic feedback control laws are presented for each driving mode: hybrid, ZEV, stop, start. All of them contain a Kalman filter which allows the estimation of the torque disturbances. Based on an electric/mechanical decoupling, the proposed approach is illustrated in the last section, focusing on a compound-split configuration.

The next step of this research program will be to size the different components of the drivetrain according to the vehicle program of demand and to evaluate fuel consumption and energy flows in the components according to various vehicle usage types.

REFERENCES

[1] M. Selogie GM : The GM 2Mode FWD Hybrid System : SAE Hybrid Vehicles Technology Symposium, San Diego, California, February 11th, 2009.

[2] J. Guldner BMW : The BMW Concept X6 ActiveHybrid within the BMW EfficientDynamics Strategy : SAE Hybrid Vehicles Technology Symposium, San Diego, California, February 11th, 2009.

[3] A. Yamanaka Toyota Motor Corp. : The Lexus Hybrids : SAE Hybrid Vehicles Technology Symposium, San Diego, California, February, 2007.

[4] R. Trigui, F. Badin, B. Jeanneret, F. Harel, R. Lallemand, J.P. Ousten INRETS, M. Castagné, M. Debest, E. Gittard, F. Vangraefshepe, V. Morel IFP, L. Baghli, A. Rezzoug, GREEN, J. Labbé, ARMINES, S. Biscaglia ADEME : Hybrid light duty vehicles evaluation program : **EVS19** Busan, Corea October 2002.

[5] A. Villeneuve, “Dual Mode Electric Infinitely Variable Transmission”, Renault, Aachener Kolloquium Fahrzeug- und Motortechnik, 2004

[6] J. Meisel, “An analytic Foundation for the Two-Mode Hybrid-Electric Powertrain with a Comparison to the Single-Mode Toyota Prius THS-II Powertrain”, Georgia Institute of Technology, SAE 2009-01-1321

[7] O. Reyss, G. Duc, P. Pognant-Gros, G. Sandou, “Robust Torque Tracking Control for E-IVT Hybrid Powertrain”, IFAC Seoul World Congress, 2008

[8] A. Chasse, P. Pognant-Gros, A. Sciarretta, , “Online Implementation of an Optimal Supervisory Control for a Parallel Hybrid Powertrain”, SAE 09SFL-0336, 2009